

# Improving uncertainty analysis of embodied energy and embodied carbon in wind turbine design

Matthew Ozoemena<sup>1</sup> · Wai M. Cheung<sup>2</sup> · Reaz Hasan<sup>2</sup>

Received: 1 August 2016 / Accepted: 26 December 2016 / Published online: 18 January 2017  
© The Author(s) 2017. This article is published with open access at Springerlink.com

**Abstract** In this paper, a method for improving uncertainty estimates of embodied carbon and embodied energy is presented and discussed. Embodied energy and embodied carbon results are the focus of this analysis due to the fact that, at the conceptual design stage, these two are the most important quantities for decision making in life cycle assessment (LCA) studies. The use of renewable and new energy sources and the development of cleaner and more efficient energy technologies will play a major role in the sustainable development of a future energy strategy. Environmental protection, economic and social cohesion and diversification and security of energy supply are highlighted by the International Energy Agency as a high priority for the development of cleaner and more efficient energy systems and promotion of renewable energy sources. In the case studies presented, better results for the baseline turbine were observed compared to turbines with the proposed technology improvement opportunities. Embodied energy and embodied carbon results for the baseline turbine show an about 50 % probability that the turbine manufacturer may have lost the chance to reduce carbon emissions and 85 % probability

that the turbine manufacturer may have lost the chance to reduce the primary energy consumed during its manufacture. The proposed approach is therefore a feasible alternative when more reliable results are desired for LCA-based design decision making.

**Keywords** Embodied energy · Embodied carbon · Technology improvement opportunities · Uncertainty · 1.5 MW wind turbine

## Nomenclature

BOM	Bill of materials
CDF	Cumulative distribution function
CFRP	Carbon fibre-reinforced plastic
CV	Coefficient of variation
DQI	Data quality indicator
EEC	Embodied energy coefficient
EF	Emission factor
HDS	Hybrid data quality indicator and statistical method
LCA	Life cycle assessment
MCS	Monte Carlo simulation
$M_{DQI}$	Mean of DQI result
$M_{HDS}$	Mean of HDS result
MRE	Mean magnitude of relative error
MW	Megawatt
$N_M$	Least number of data points required
$N_{MD}$	Least number of required data points for individual parameter distribution estimation
$N_P$	Number of parameters involved
NREL	National Renewable Energy Laboratory
PDF	Probability distribution function
TIO	Technology improvement opportunities

**Electronic supplementary material** The online version of this article (doi:10.1007/s00170-016-9972-7) contains supplementary material, which is available to authorized users.

✉ Wai M. Cheung  
wai.m.cheung@northumbria.ac.uk

<sup>1</sup> Warwick Manufacturing Group, International Institute for Product and Service Innovation, The University of Warwick, Coventry CV4 7AL, UK

<sup>2</sup> Faculty of Engineering and Environment, Department of Mechanical and Construction Engineering, Northumbria University, Newcastle Upon Tyne NE1 8ST, UK

## 1 Introduction

There is a persistent need to hasten the expansion of innovative energy technologies with the aim of addressing the global challenges of climate change, sustainable development and clean energy. To achieve the envisioned emission reductions, the International Energy Agency (IEA) has undertaken efforts to develop global technology roadmaps, in close consultation with industry and under international guidance [1]. Wind energy, like other renewable resource-based power technologies, is widely available globally and can contribute to reduced dependence on imported energy and hence improves security of supply. Wind power improves energy diversity and safeguards against fossil fuel price unpredictability, thus stabilizing electricity generation costs in the long term [2].

All energy systems for converting energy into usable forms have environmental impacts associated with them [3–6]. The production of renewable energy sources involves the consumption of energy and natural resources as well as the release of pollutants like every other production process [7–12]. Life cycle assessment (LCA) is a popular way of measuring the environmental impacts and energy performance of wind energy [3, 13]. Oebels et al. [14] state that estimation of embodied energy and embodied carbon is a significant aspect of life cycle assessments. Hammond and Jones [15] defined embodied carbon (energy) of a material as the total carbon released (primary energy consumed) over its life cycle. It has however become common practice to specify the embodied carbon (energy) as ‘cradle-to-gate’, which includes all carbon (energy—in primary form) until the product leaves the factory gate [15].

Embodied carbon and energy are usually estimated deterministically using single fixed point values to generate single fixed point results [16]. Lack of detailed production data and production process differences result in considerable variations in emission factor (EF) and embodied energy coefficient (EEC) values among different life cycle inventory (LCI) databases [17, 18]. Hammond and Jones [15] note that a comparison of selected values in these inventories would show a lot of similarities but also several differences. These variations known as ‘data uncertainty’ significantly affects the results of embodied energy and embodied carbon LCA [19]. Decision makers have different attitudes towards uncertainty making information on uncertainty in LCA to be highly sought after [17, 19]. The analysis of data uncertainty is therefore a significant improvement to the deterministic approach because it improves decision making by providing more information [8, 20, 21].

Stochastic modelling, analytical uncertainty propagation, interval calculations, fuzzy data sets and scenario modelling are well understood and generally accepted methods normally used for uncertainty propagation in LCA studies [18]. Stochastic and scenario modelling methods were used to propagate uncertainty in the wind energy LCA studies surveyed.

Kabir et al. [20], Fleck and Huot [22] and Khan et al. [23] use the Monte Carlo analysis method which performs well for cases when reliability of the uncertainty estimate is not paramount. Due to the ‘rule of thumb’ nature of this method, it may lead to inaccurate results making it a key limitation of this approach. For more reliable results, the determination of significant contributors to uncertainty, selection of appropriate distributions and maintaining correlation between parameters are identified in Lloyd and Ries [16] as areas requiring better understanding. In this study, an improved hybrid data quality indicator and statistical (HDS) method for improving uncertainty estimates is presented and discussed. The method employs the same basics as the Monte Carlo analysis but has a key distinction, aiming at removing the drawback of the Monte Carlo analysis method by employing a stochastic pre-screening process to determine the influence of parameter contributions. The overall aim of this study is to present an analysis of potential technological advancements for a 1.5-MW wind turbine using a hybrid stochastic method to improve uncertainty estimates of embodied energy and embodied carbon. This approach can be a valuable tool for design scheme selection aiming to find an embodied energy and embodied carbon saving design when information on uncertainty is required for design decision making in LCA. The organization of the content of this paper is as follows: Section 2 explains the fundamentals of the methodology. Section 3 contains a description of the case studies and results. Section 4 and 5 are the discussion and conclusions.

## 2 Methodology

### 2.1 Estimation of embodied energy and embodied carbon

Ortiz et al. [24] and Wang and Sun [25] express embodied carbon and embodied energy mathematically as:

$$\text{Embodied carbon} = \sum_{i=1}^n Q_i \times \text{EF}_i \quad (1)$$

$$\text{Embodied energy} = \sum_{i=1}^n Q_i \times \text{EEC}_i \quad (2)$$

Where,

$Q_i$	Quantity of material $i$
$\text{EEC}_i$	Embodied energy coefficient of material $i$
$\text{EF}_i$	Emission factor of material $i$

### 2.2 Quantitative DQI method

This method transforms aggregated data quality indicator (DQI) scores into probability distributions to enable quantification of uncertainty using predefined uncertainty

parameters. The DQI scores use a single rating to measure the overall quality of each data element. This rating is based upon a scale of 1 to 5, with a 1 representing the worst quality (maximum uncertainty) and a 5 representing the best quality (minimum uncertainty) as shown in Table 1. These qualitative assessments are then used to parameterize the probability density function of a beta random variable  $x$  as shown in Eq. (3):

$$f(x; \alpha, \beta, a, b) = \left[ \frac{1}{b-a} \right] \left\{ \frac{\Gamma(\alpha + \beta)}{\Gamma(\alpha)\Gamma(\beta)} \right\} \left[ \frac{x-a}{b-a} \right]^{\alpha-1} \left[ \frac{b-x}{b-a} \right]^{\beta-1} \quad \text{for } (a \leq x \leq b); \quad (3)$$

where  $\alpha$  and  $\beta$  are shape parameters of the distribution,  $a$  and  $b$  are designated range end points and  $\Gamma$  is the gamma function. The beta function is used due to the fact that ‘the range of end points and shape parameters allow practically any shape of probability distributions to be represented’.

## 2.3 HDS approach

The HDS approach involves four steps: (i) quantitative DQI with Monte Carlo simulation (MCS), (ii) categorization of parameters, (iii) detailed estimation of probability distributions for parameters and (iv) final MCS calculation. The parameter characterization identifies the critical parameters based on the influence and degree of uncertainty of the parameters. The final stochastic results are generated through a MCS calculation.

### 2.3.1 Quantitative DQI with MCS

This step begins with assessing data quality using the qualitative DQI approach. All parameters used for the deterministic calculations are assessed using the DQI matrix. After calculation of the aggregated DQI scores, probability distributions for the parameters are determined using the transformation matrix (Table 2) and used as inputs for the MCS to carry out an influence analysis.

### 2.3.2 Categorization of parameters

The degree of parameter uncertainty is obtained in the data quality assessment process. Parameters are consequently classified into groups of four with DQI scores belonging to the intervals of (1, 2), (2, 3), (3, 4) and (4, 5), respectively. The group containing parameters with DQI scores within the interval of (1, 2) and (2, 3) shows the highest uncertainty, and the group with parameters scored within the interval of (3, 4) and (4, 5) represents the highest certainty. The influence of the

**Table 1** Data quality indicator (DQI) matrix based on Weidema and Wesnes [26] and NETL [27]

Quality scale						
Data quality indicators		1	2	3	4	5
Data representativeness	Representativeness unknown or incomplete data from insufficient sample of sites and/or for a shorter period	Representative data from a smaller number of sites for a shorter period or incomplete data from an adequate number of sites and periods	Representative data from an adequate number of sites but for a shorter period	Representative data from a smaller number of sites but for an adequate period	Representative data from a sufficient sample of sites over an adequate period to even out normal fluctuations	
Age		≥15 years old	<15 years old	<10 years old	<6 years old	<3 years old
Acquisition method	Non-qualified estimation	Qualified estimation by experts	Calculated data partly based on assumptions	Calculated data based on measurements	Directly measured data	
Supplier independence	Unverified information from enterprise interested in the study	Unverified information from irrelevant enterprise	Independent source but based on unverified information	Verified data from enterprise with interest in the study	Verified data from independent source	
Geographical correlation	Unknown area	Data from an area with slightly similar production conditions	Data from an area with similar production conditions	Average data	Data from the exact area	
Technological correlation	Data from process related of company with different technology	Data from process related of company with similar technology	Data from process studied of company with different technology	Data from process studied of company with similar technology	Data from process studied of the exact company with the exact technology	
Rule of inclusion/exclusion	Unknown	Non-transparent on exclusion but specification of inclusion	Transparent, not-justified, uneven application	Transparent, justified, uneven application	Transparent, justified, homogeneous application	

**Table 2** Transformation matrix based on Weidema and Wesnæs [26], and Canter et al. [28]

Aggregated DQI scores	Beta distribution function	
	Shape parameters ( $\alpha, \beta$ )	Range end points ( $\pm\%$ )
5.0	(5, 5)	10
4.5	(4, 4)	15
4.0	(3, 3)	20
3.5	(2, 2)	25
3.0	(1, 1)	30
2.5	(1, 1)	35
2.0	(1, 1)	40
1.5	(1, 1)	45
1.0	(1, 1)	50

input parameters on the results is determined via correlation analysis as given in Eq. 4.

$$r_{p,q} = 1 - \left[ \frac{6}{(N^3 - N)} \right] \sum_{i=1}^N [\text{rank}(p_i) - \text{rank}(q_i)]^2 \quad (4)$$

where  $\text{rank}(p_i)$  and  $\text{rank}(q_i)$  are the ranks of  $p_i$  and  $q_i$  among the  $N$  tuple data points. The contribution of a single uncertain input parameter to the result of an impact category is calculated according to Eq. 5.

$$IA_{p,q} = r_{p,q}^2 \left[ \sum_p r_{p,q}^2 \right]^{-1} \times 100\% \quad (5)$$

where  $IA_{p,q}$  is the influence of input parameter  $p$  to output  $q$ , and  $r_{p,q}$  is the rank-order correlation factor between input  $p$  and the output  $q$ .

### 2.3.3 Detailed estimation of probability distributions for parameters

The statistical method is applied to the process of probability distributions fitting for the critical parameters identified. Kolmogorov-Smirnov goodness of fit test (K-S test) is used to fit data samples due to its sensitivity to variations in distribution types in terms of shape and scale parameters and its intrinsic exactness compared to other goodness of fit tests, e.g. chi-square test and Anderson-Darling (A-D) test. The statistic for the K-S test is defined as:

$$D = \max_{1 \leq i \leq N} \left[ F(Y_i) - \frac{i-1}{N}, \frac{i}{N} - F(Y_i) \right] \quad (6)$$

where  $F$  is the theoretical cumulative distribution of the distribution that is being tested, and  $N$  means  $N$  ordered data points  $Y_1, Y_2, \dots, Y_N$ . For the non-critical parameters of lower uncertainty and influence, their probability distributions are

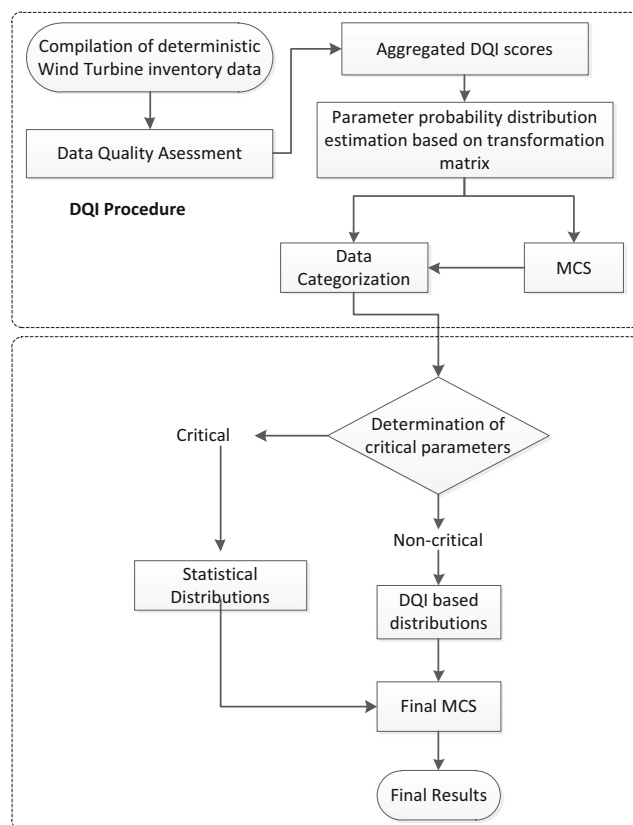
estimated using the transformation matrix and the DQI scores, making the HDS approach more economical and efficient compared to the statistical method.

### 2.3.4 Final MCS calculation

The stochastic results are calculated by MCS algorithm, according to the input and output relationships, using the intricately estimated probability distributions for the parameters as the inputs. Figure 1 shows the procedure for the HDS approach.

### 2.3.5 Validation

To validate the HDS approach, comparisons are made between the pure DQI, statistical and HDS methods. The measurements mean magnitude of relative error (MRE) (Eq. (7)) and coefficient of variation (CV) (Eq. (8)) are used to measure the differences in the results of the pure DQI and HDS. CV is an indicator that shows the degree of uncertainty and measures the spread of a probability distribution. A large CV value indicates a wide distribution spread. The data requirements are also used to compare the HDS with the statistical method, as large enough sample size needs to be satisfied during parameter distribution estimation. The least number of data

**Fig. 1** Procedure of HDS approach [18]

points necessary for estimating parameter distributions in each method is calculated (Eq. (9)) and compared.

$$\text{MRE} = \frac{(M_{\text{HDS}} - M_{\text{DQI}})}{M_{\text{HDS}}} \times 100\% \quad (7)$$

where  $M_{\text{DQI}}$  is the mean of the DQI results and  $M_{\text{HDS}}$  is the mean of the HDS results

$$\text{CV} = \frac{\text{SD}}{M} \quad (8)$$

where  $M$  is the mean and SD is the standard deviation

$$N_{\text{M}} = N_{\text{MD}} \times N_{\text{P}} \quad (9)$$

where  $N_{\text{M}}$  is the least number of data points required,  $N_{\text{MD}}$  is the least number of required data points for individual parameter distribution estimation and  $N_{\text{P}}$  is the number of parameters involved.

### 3 Case study and result analysis

#### 3.1 Background of the case study

Figure 2 illustrates a 1.5-MW wind turbine which is used as a case study for potential technological advancement analyses. The embodied energy and embodied carbon analyses are based on improvements to the blades, generator and tower. This is due to the fact that different materials are used in these components. The projections of future technological designs as a result of research and scientific developments are based on National Renewable Energy

Laboratory (NREL) [29] 1.5-MW wind turbine technology forecasting studies. These are further explained in Cohen et al. [30] and Lantz et al. [31] and provided the basis for modelling future inventory changes in this study. As such, an Enercon E-66 1.5 MW turbine was chosen as it shares similar technical characteristics to the NREL baseline turbine. The bill of materials (BOM) of the Enercon E-66 can be seen in the Appendix (Table 8) [32]. Embodied energy and embodied carbon are considered the main measure of environmental impact measurement.

#### 3.2 Technology improvement opportunities (TIOs)

According to Cohen et al. [30] and Lantz et al. [31], identification of TIOs relied on judgements and technical insights of the senior research staff at the Sandia National Laboratories and National Wind Technology Centre at the NREL. The design of wind turbines is a matter of continuous compromise between the rival demands of greater energy productivity, lower cost, increased durability and lifetime and maintenance cost. These are the designers' trade-offs captured in the model. The outcome of the details of the TIOs is summarized in Table 3.

#### 3.3 Mass scaling equations

To generate the material quantities for the different TIOs, information and scaling equations were taken from the NREL study of Fingersh et al. [33]. The report contained information about how the various components could be scaled using semi-empirical formulas. The equations used in this study are defined in Table 4 as well as an indication as to where they were employed.

### 4 Analysis and results

#### 4.1 Quantitative DQI transformation

To appropriately transform the qualitative assessment results to the equivalent quantitative probability density functions, Wang and Shen [18] suggest that the aggregated DQI scores be approximated to the nearest nominal value so as to use the transformation matrix. Figure 3 shows the obtained aggregated DQI scores. The quantitative DQI procedure was then used to transform the scores into beta distributions. Most of the data used in the study are of good quality and were taken from the same data source and hence showed identical transformed beta function parameters ( $\alpha = 4$ ,  $\beta = 4$ ), the same DQI score of 4.5 and range end points of 15 %. The exceptions were cast iron EF, cast iron EEC and gear oil EEC showing DQI scores of 3.5, transformed beta function parameters of

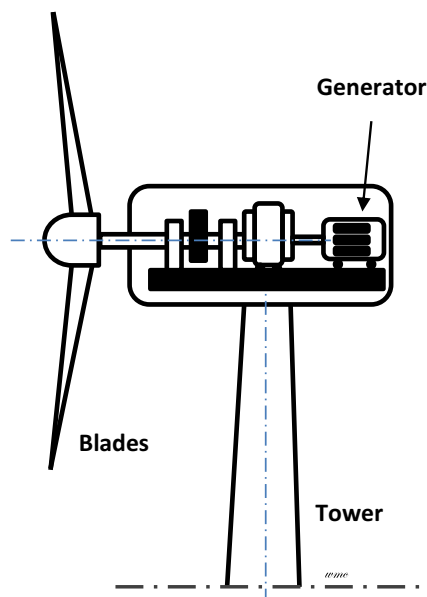


Fig. 2 Potential wind turbine performance improvements



**Table 3** Potential contributions to wind turbine performance improvement

Performance improvement	Technology pathway	Description
TIO 1	Advanced (enlarged) rotors	Stiffer carbon fibre materials allowing for 25 % rotor growth and 2 % reduction in tower mass
TIO 2	Advanced tower concepts	New tower concepts using carbon fibre materials and power production at 100 m compared to 65 m
TIO 3	Drivetrain improvements	Permanent magnet generators that use permanent magnets instead of copper wound rotors
TIO 4	Fully combined TIOs	A combination of all the potential technological advancements

( $\alpha = 2$ ,  $\beta = 2$ ) and range end points of 25 % making them more uncertain.

#### 4.2 Parameter categorization and probability distributions estimation

Results of the influence analysis (10,000 iterations MCS) showing the two parameters contributing the most to the resulting uncertainty are presented in Table 5. Two parameters, steel and carbon fibre-reinforced plastic (CFRP), demonstrated the largest influence on the final resulting uncertainty of embodied energy and embodied carbon across all case studies. For the parameters with a lesser contribution to the final resulting uncertainty, there were variations across all case studies. Normal concrete and CFRP show the lesser contribution for embodied carbon, while steel (no alloy), CFRP and cast iron show the lesser contribution for embodied energy across all case studies. Combining these results, further analysis was conducted on the two identified parameters for each test case using the statistical method, while the values for the remaining parameters were obtained from the quantitative DQI. Probability distributions were thus fitted to data points collected manually from literature. Results of the estimated probability distributions for the different parameters are presented in Table 6.

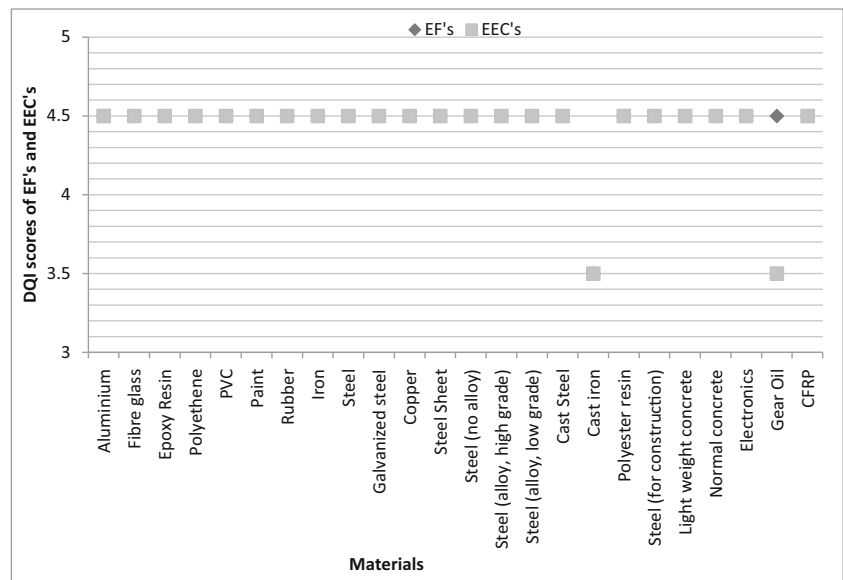
#### 4.3 Stochastic results comparison of DQI and HDS approaches for the different case studies

Embodied carbon and embodied energy stochastic results (10,000 iterations MCS) using the pure DQI and HDS methods were obtained for the baseline turbine and TIOs 1–4; the results of which are presented in this section. Results for each case study are presented graphically through probability distribution functions (PDFs) and cumulative distribution functions (CDFs) in Figs. 4, 5 and 6. In addition to these figures, MRE and CV values were also calculated. A summary of the relevant information is provided in Table 7. Probability distributions were fitted to the stochastic results according to K-S test. From the PDFs (Figs. 4a, c, e, g, 5a, c, e, g and 6a, c), it can be seen that the mean value and standard deviation for the pure DQI and HDS results show rather different dispersion across all the case studies. The CV values of the HDS results are on average about six times larger than the CV values of the pure DQI results. In terms of MRE, the difference observed between the HDS and pure DQI results indicates that the HDS method captures more possible outcomes compared to the pure DQI. The differences between the deterministic, pure DQI and HDS results can be inferred from the CDFs (Figs. 4b, d, f, h, 5b, d, f, h and 6b, d). Figure 4b for example shows that, for the HDS result, about 85 % of the likely resulting values are smaller than the deterministic result

**Table 4** Mass scaling equations for the different components

Component	Equation	Description
Blade	<ul style="list-style-type: none"> <li>Baseline: Mass = <math>0.1452 \times R^{2.9158}</math> per blade</li> <li>Advanced: Mass = <math>0.4948 \times R^{2.53}</math> per blade</li> </ul>	Where $R$ = rotor radius. The advanced blade mass relationship follows products developed by a wind turbine blade manufacturer which 'represents combinations of technology enhancements that may not/may include carbon and takes advantage of a lower weight root design'
Tower	<ul style="list-style-type: none"> <li>Baseline: Mass = <math>0.3973 \times \text{swept area} \times \text{hub height} - 1414</math></li> <li>Advanced: Mass = <math>0.2694 \times \text{swept area} \times \text{hub height} + 1779</math></li> </ul>	The baseline case is based on conventional technology for 2002, while the advanced case represents advanced technologies including reduced blade solidity in conjunction with higher tip speeds, flap-twist coupling in the blade and tower feedback in the control system
Generator	<ul style="list-style-type: none"> <li>Mass = <math>10.51 \times \text{machine rating}^{0.9223}</math></li> </ul>	A generator mass calculation for the medium-speed permanent magnet generator design was based on machine power rating in kW

**Fig. 3** Aggregated DQI scores for emission factors and embodied energy coefficients



obtained, while for the DQI result, 50 % of the possible results are smaller than the deterministic result. Figure 4d also shows that for the HDS result, about 15 % of the likely results are smaller than the deterministic result, while for the DQI result, half of the possible resulting values are lesser than the deterministic result. A comprehensive analysis of the implications of these results is presented in Section 5.

#### 4.4 Comparison of statistical and HDS methods in terms of data requirements

It can be seen that from the procedure of the HDS approach which categorizes critical parameters and uses the statistical method to estimate their probability distributions, the reliability of the HDS results is not greatly jeopardized. According to Wang and Shen [18], the statistical method requires at least 30 data points to estimate one parameter distribution. Hence, in this study, 46 parameter distributions are required to be estimated for each case study with the exception of TIO 1 which

has 48 parameter distributions for estimation. If the statistical method was implemented, at least 1380 data points would have been required for the estimation for each case study. That would mean 6900 data points across all the case studies. This would have been very time consuming even if all the data points were available. The HDS requires only 120 data points for each case study (600 data points across all the case studies), thus reducing the data requirements by approximately 91 %. This avoids the issue associated with lack of data and saves cost and time without seriously compromising the reliability of the HDS results as the critical parameters identified explain the majority (at least 69 %) of the overall uncertainty across all the case studies.

## 5 Discussion

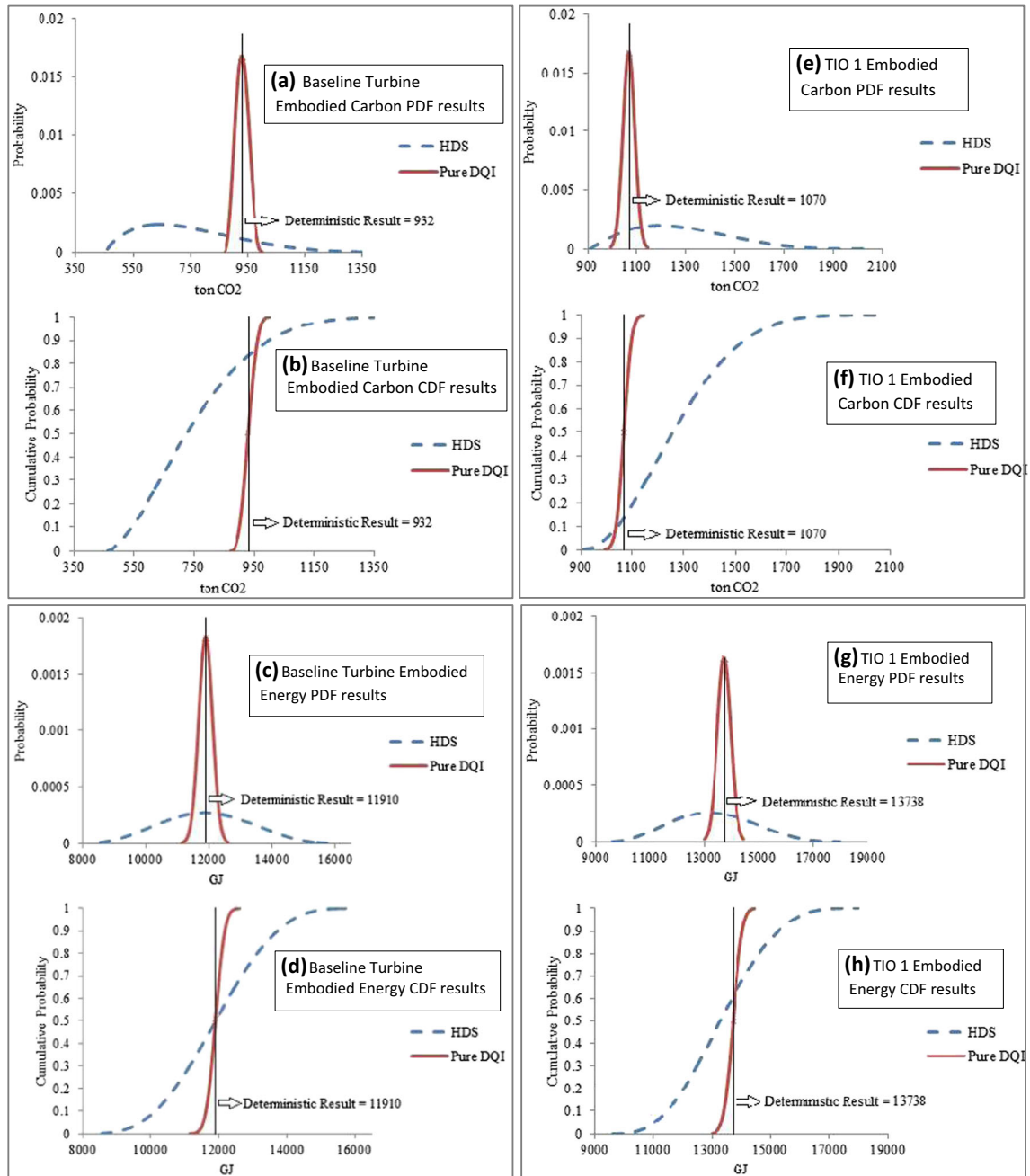
This study uses the HDS approach to provide insight into potential technological advancements for a 1.5-MW wind

**Table 5** Influence analysis

	Embodied carbon	Influence (%)	Embodied energy	Influence (%)
Baseline turbine	Steel EF	78	Steel EEC	62
	Normal concrete EF	9	Steel (no alloy) EEC	9
TIO 1	Steel EF	66	Steel EEC	47
	CFRP EF	17	CFRP EEC	22
TIO 2	CFRP EF	99	CFRP EEC	97
	Normal concrete EF	0.3	Steel (no alloy) EEC	0.7
TIO 3	Steel EF	81	Steel EEC	66
	Normal concrete EF	8	Cast iron EEC	9
TIO 4	CFRP EF	98	CFRP EEC	97
	Normal concrete EF	0.6	Steel (no alloy) EEC	0.5

**Table 6** Probability distribution estimation for the different parameters

Parameter	Probability distribution	Mean	Data points collected
Steel EF	Beta (1.24, 4.47)	1.73 t CO <sub>2</sub> /t	30
Steel EEC	Beta (2.96, 4.16)	25.87 GJ/t	31
Normal concrete EF	Beta (20.8, 87.7)	0.11 t CO <sub>2</sub> /t	31
Steel (no alloy) EEC	Beta (48.6, 62.3)	25.57 GJ/t	31
CFRP EF	Beta (3.16, 2.2)	52.4 t CO <sub>2</sub> /t	31
CFRP EEC	Beta (2.13, 6.23)	191.3 GJ/t	31
Cast iron EEC	Beta (36.6, 75.2)	35.4 GJ/t	31

**Fig. 4** a–h Results of baseline and TIO 1 wind turbines



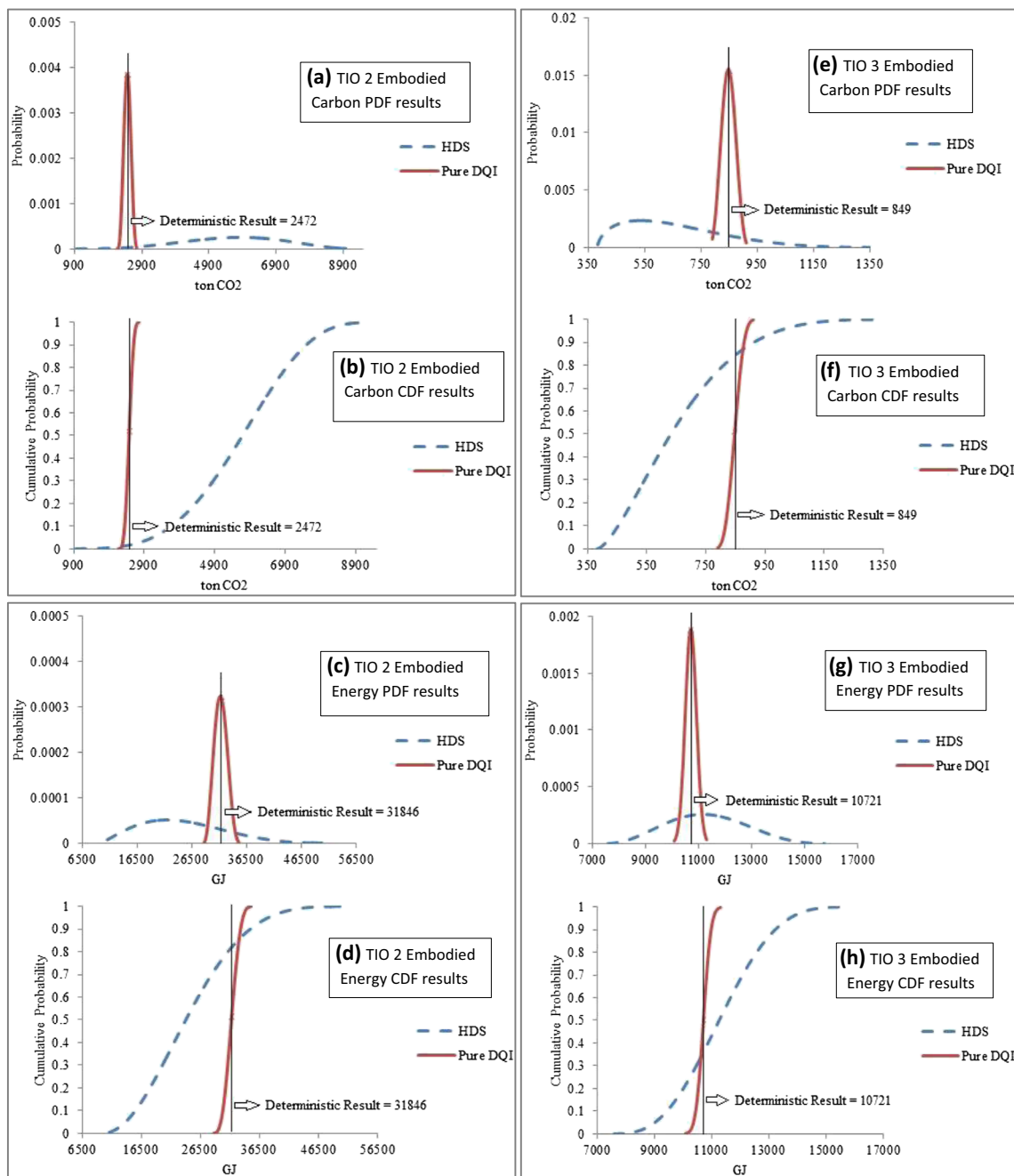


**Fig. 5** a–h Results of TIO 2 and TIO 3 wind turbines

turbine and makes evident how variability of input parameters results in differing embodied energy and embodied carbon results. Analysing the parameter categorization revealed that EFs and EECs for steel, normal concrete, steel (no alloy), CFRP and cast iron accounted for the majority of output uncertainty in embodied energy and embodied carbon results. Steel is the main material component of the baseline wind turbine, followed by normal concrete. The large contribution of steel is probably attributed to the wide EF and EEC distributions assigned to steel in the probability distribution estimations. Therefore, any uncertainty in steel EFs and EECs is

magnified by the sheer mass of steel. Interestingly, although the mass of concrete (575 t) is greater than the mass of steel (144 t), steel EFs and EECs contribute more to the overall uncertainty of embodied energy and embodied carbon. For example, the EFs of steel range from 0.01 to 5.93 t CO<sub>2</sub>/t steel, whereas values for concrete range from 0.02 to 0.28 t CO<sub>2</sub>/t. Likewise, the EECs for steel range from 8.6 to 51 GJ/t steel, whereas values for steel (no alloy) range from 8.3 to 50.7 GJ/t. Concrete generally is much less emission intensive than steel for CO<sub>2</sub> and, hence, is a lesser contributor to the sensitivity of embodied carbon. It can also be observed that while normal

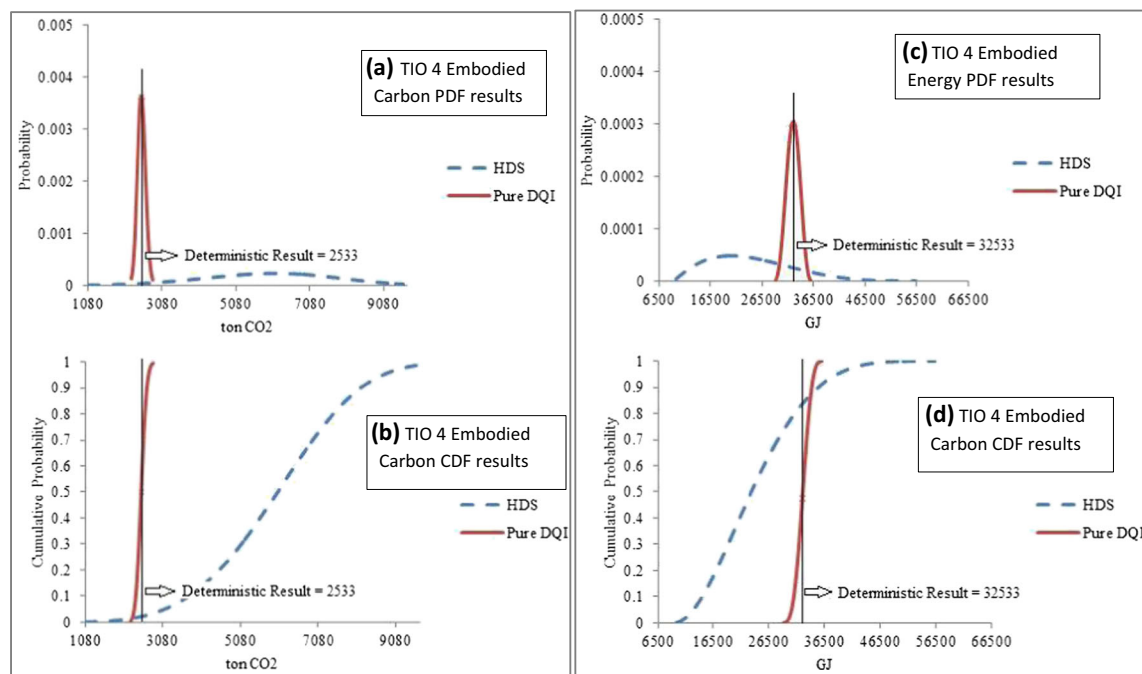


**Fig. 6** a–d Results of TIO 4 wind turbine

concrete EF and steel (no alloy) EEC contribute 9 % each, steel EF and steel EEC contribute 78 and 62 %, respectively, to the resulting uncertainty. This highlights the influence of the wider distribution range of steel (no alloy) EEC compared to normal concrete EF. Due to the wide distribution ranges and mass of steel, variations in steel EFs and EECs have significantly more impact on the embodied energy and embodied carbon uncertainty even though there is normally more concrete than steel.

For TIO 1, normal concrete and steel are also major material components of the turbine with 575 and 141 t, respectively. However CFRP contributes considerably to the resulting uncertainty, second only to steel, while having a mass of 8.6 t (1 % of the turbine mass). This can be attributed to CFRP being very emission and energy intensive. The EFs for CFRP range from 11.2 to 86.3 t CO<sub>2</sub>/t CFRP, compared to the steel EF range of 0.01–5.93 t CO<sub>2</sub>/t steel. Similarly, the EECs for CFRP range from 55 to 594 GJ/t CFRP compared to the steel EEC range of 8.6–51 GJ/t steel. Hence, due to the wide distribution ranges in CFRP EF and EEC input factors, despite its minor mass contribution, CFRP has a considerable impact on the uncertainty of the embodied energy and embodied carbon. For TIO 2, the major material components are normal concrete and CFRP with 575 and 88.5 t, respectively. Despite being second in mass to steel, CFRP contributes 99 and 97 % of the resulting uncertainty for embodied carbon and embodied energy, respectively. This is attributed to its high emission intensity, energy intensity and wide distribution ranges. As a result, CFRP significantly impacts the uncertainty of the embodied energy and embodied carbon.

Normal concrete and steel are the major material components in TIO 3 with 575 and 144 t, respectively. The contribution of steel to the final resulting uncertainty is again attributed to the range of values of EFs and EECs. Cast iron has a mass of 21 t and EEC values ranging between 11.7 and 94.5 GJ/t which could explain the lesser contribution of steel EEC to the resulting uncertainty for the embodied energy (66 %) compared to the steel EF contribution for embodied carbon (81 %). For TIO 4, the major material components are normal concrete with 575 t and CFRP with 97 t. CFRP contributes 98 and 97 % of the resulting uncertainty for embodied carbon and embodied energy, respectively. Again, the sheer tonnage of CFRP combined with its high emission and energy intensity and wide distribution ranges result in its significant contribution to the resulting uncertainty of the embodied energy and embodied carbon.

The intention of quantifying uncertainty with the HDS approach in this study is to provide more information for the decision-making process. From the above case studies, it is assumed that the deterministic result is used for design scheme selection aiming to find an embodied carbon and embodied energy-saving design. The baseline turbine is commercially available; hence, in terms of embodied carbon, there is an about 85 % probability (Fig. 4b) Enercon saved carbon emissions with the design. Thus, it is a good design in terms of embodied carbon savings. In terms of embodied energy, there is a 50 % probability (Fig. 4d) Enercon reduced the primary energy consumed during manufacture with the design. The TIOs proposed in this study are design concepts. Hence, for TIO 1 in terms of embodied carbon, there is an about 15 %

**Table 7** Pure DQI and HDS results for the different case studies

	Embodied carbon		Embodied energy	
	DQI	HDS	DQI	HDS
Baseline turbine	Beta distribution (4.5, 5.3) $\mu = 932 \text{ t CO}_2$ $\sigma = 22 \text{ t CO}_2$ CV = 0.02	Beta distribution (1.8, 5.1) $\mu = 733 \text{ t CO}_2$ $\sigma = 183 \text{ t CO}_2$ CV = 0.25 MRE = 27 %	Normal distribution $\mu = 11,909 \text{ GJ}$ $\sigma = 218 \text{ GJ}$ CV = 0.02	Beta distribution (4.4, 4.7) $\mu = 11,831 \text{ GJ}$ $\sigma = 1424 \text{ GJ}$ CV = 0.12 MRE = 1 %
TIO 1	Normal distribution $\mu = 1070 \text{ t CO}_2$ $\sigma = 24 \text{ t CO}_2$ CV = 0.02	Beta distribution (2.3, 5.2) $\mu = 1269 \text{ t CO}_2$ $\sigma = 188 \text{ t CO}_2$ CV = 0.15 MRE = 16 %	Normal distribution $\mu = 13,735 \text{ GJ}$ $\sigma = 244 \text{ GJ}$ CV = 0.02	Beta distribution (3.8, 4.7) $\mu = 13,276 \text{ GJ}$ $\sigma = 1469 \text{ GJ}$ CV = 0.11 MRE = 3.5 %
TIO 2	Beta distribution (5, 5.3) $\mu = 2475 \text{ t CO}_2$ $\sigma = 96 \text{ t CO}_2$ CV = 0.04	Beta distribution (5.8, 4.1) $\mu = 5521 \text{ t CO}_2$ $\sigma = 1654 \text{ t CO}_2$ CV = 0.3 MRE = 55 %	Beta distribution (4.1, 4.8) $\mu = 31,822 \text{ GJ}$ $\sigma = 1166 \text{ GJ}$ CV = 0.04	Beta distribution (2.4, 4.7) $\mu = 24,687 \text{ GJ}$ $\sigma = 7608 \text{ GJ}$ CV = 0.3 MRE = 29 %
TIO 3	Beta distribution (5.3, 5.7) $\mu = 849 \text{ t CO}_2$ $\sigma = 22 \text{ t CO}_2$ CV = 0.03	Beta distribution (1.6, 4.6) $\mu = 647 \text{ t CO}_2$ $\sigma = 185 \text{ t CO}_2$ CV = 0.29 MRE = 31 %	Normal distribution $\mu = 10,722 \text{ GJ}$ $\sigma = 211 \text{ GJ}$ CV = 0.02	Beta distribution (3.8, 4.8) $\mu = 11,249 \text{ GJ}$ $\sigma = 1474 \text{ GJ}$ CV = 0.13 MRE = 5 %
TIO 4	Gamma distribution (529, 4.8) $\mu = 2529 \text{ t CO}_2$ $\sigma = 108 \text{ t CO}_2$ CV = 0.04	Weibull distribution (3.96, 6621) $\mu = 5988 \text{ t CO}_2$ $\sigma = 1746 \text{ t CO}_2$ CV = 0.29 MRE = 58 %	Beta distribution (4.7, 4.5) $\mu = 32,503 \text{ GJ}$ $\sigma = 1304 \text{ GJ}$ CV = 0.04	Beta distribution (2.1, 4.6) $\mu = 24,299 \text{ GJ}$ $\sigma = 8419 \text{ GJ}$ CV = 0.35 MRE = 33 %

probability (Fig. 4f) that a manufacturer will be able to reduce carbon emissions with this design. Hence, it is not a good design for embodied carbon savings. In terms of embodied energy, there will be a 60 % (Fig. 4h) probability that a manufacturer will be able to reduce the primary energy consumed. This design thus performs better in terms of embodied energy savings.

For TIO 2, results show that for embodied carbon, there is a 1 % probability (Fig. 5b) a manufacturer will be able to reduce carbon emissions therefore making it a bad design. The embodied energy results show that there is about an 85 % probability (Fig. 5d) a manufacturer will be able to reduce the primary energy consumed making it a good design in terms of embodied energy savings. The huge difference in the results, despite CFRP's contribution of 99 % and 97 % to the resulting uncertainty for embodied carbon and embodied energy, can be attributed to the differences in distribution ranges of steel (no alloy) and normal concrete EEC and EF input factors. EEC values of steel (no alloy) range from 8 to 51 GJ/t compared to EF values of concrete that range from 0.02 to 0.28 t CO<sub>2</sub>/t. This highlights how variations in EF and

EEC values significantly affect results of embodied carbon and embodied energy LCA.

Results show that for TIO 3, there will be an about 85 % probability (Fig. 5f) that a manufacturer will be able to reduce carbon emissions with this design. It is therefore a good design in terms of embodied carbon savings. For embodied energy, results show that there is about a 35 % probability (Fig. 5h) a manufacturer will be able to reduce the primary energy consumed. This design therefore performs better in terms of embodied carbon savings. For TIO 4 in terms of embodied carbon, there would be about a 1 % probability (Fig. 6b) that a manufacturer will be able to reduce carbon emissions making it a bad design. For embodied energy, results show the probability that a manufacturer will be able to reduce the primary energy consumption is about 85 % (Fig. 6d) making it a good design in terms of embodied energy savings. The difference in the results, despite CFRP's contribution of 98 and 97 % to the resulting uncertainty for embodied carbon and embodied energy, could again be attributed to reasons described in TIO 2. From the results of the different case studies, more information was gained for decision making using the HDS approach

compared to the DQI. The confidence level which is the important factor for decision making was observed, and it can be seen that the DQI approach gave more conservative results, consistent with conclusions in Venkatesh et al. [34], Tan et al. [21] and Lloyd and Ries [16], which could lead to unreliable decisions. For example, the results for all the case studies showed the pure DQI approach giving a 50 % probability making any decisions made using the pure DQI quite unreliable. Thus, the HDS approach is a useful alternative for the evaluation of deterministic wind turbine embodied energy and embodied carbon LCA results when knowledge of the data uncertainties is required. The baseline wind turbine therefore performs best in terms of an embodied energy and embodied carbon-saving scheme.

## 6 Conclusions and further work

This paper demonstrates a method for improving the uncertainty estimates of embodied energy and embodied carbon for wind turbines at the design stage. Based on the study described in this work, the following remarks can be made:

- In order to quantify the uncertainty in embodied carbon and embodied energy, the HDS method has distinct advantages over deterministic approaches as is evidenced by reference to a 1.5-MW baseline wind turbine and four variants of technology improvement opportunities as described in NREL resources. Overall, the baseline turbine appears to have the lowest environmental impact compared to the TIOs and hence represents a suitable choice for potential investment.
- The HDS approach far outperforms the DQI approach by reference to MRE and CV results in evaluating the embodied energy and embodied carbon. Hence, a strong argument can be made to advocate the use of HDS over DQI when accuracy and uncertainty estimate is paramount.
- Uncertainty in the results largely depends on the distribution ranges of input parameters, which is magnified by the mass of materials. Hence, it has been shown that a strong relationship exists between material mass and input parameter distribution ranges.
- It is relevant to note here that the current study is based on the wind turbine technology of 2002, and it is fully recognized that technology has changed significantly over the past one and a half decade. However, the methodology which has been presented in this paper is novel and can be applied to modern wind turbines had the detailed data been available. However, it is likely that there will be a gap of several years before reliable commercial data are made available to the open literature due to commercial secrecy.

Future studies may conduct uncertainty analysis using the HDS approach to analyse these technological changes in the development of newer wind turbines and other renewable technologies. This would be another excellent application for the HDS methodology. It will also be interesting to study the consequence of variations for BOM (Table 7) in order to see the impact on uncertainty estimates of embodied energy and embodied carbon. Such a study would however require abundant sources of aggregated data for the material quantities of a wind turbine. Finally, the proposed method can easily be adapted to conduct further studies on different designs of wind turbines as well as other emerging renewable energy technologies at the concept design stage.

**Open Access** This article is distributed under the terms of the Creative Commons Attribution 4.0 International License (<http://creativecommons.org/licenses/by/4.0/>), which permits unrestricted use, distribution, and reproduction in any medium, provided you give appropriate credit to the original author(s) and the source, provide a link to the Creative Commons license, and indicate if changes were made.

## References

1. IEA (2009) Technology roadmap: wind energy. Available at [http://www.iea.org/publications/freepublications/publication/wind\\_roadmap.pdf](http://www.iea.org/publications/freepublications/publication/wind_roadmap.pdf) (accessed on 26-07-2016)
2. IEA (2013) Technology roadmap: wind energy. Available at [https://www.iea.org/publications/freepublications/publication/Wind\\_2013\\_Roadmap.pdf](https://www.iea.org/publications/freepublications/publication/Wind_2013_Roadmap.pdf) (accessed on 26-07-2016)
3. Davidsson S, Höök M, Wall G (2012) A review of life cycle assessments on wind energy systems. *The Int J Life Cycle Assess* 17(6):729–742. doi:10.1007/s11367-012-0397-8
4. He B, Tang W, Wang J, Huang S, Deng Z, Wang Y (2015) Low-carbon conceptual design based on product life cycle assessment. *The Int J Adv Manuf Technol* 81(5–8):863–874. doi:10.1007/s00170-015-7253-5
5. Aso R, Cheung WM (2015) Towards greener horizontal-axis wind turbines: analysis of carbon emissions, energy and costs at the early design stage. *J Clean Prod* 87:263–274. doi:10.1016/j.jclepro.2014.10.020
6. Simons PJ, Cheung WM (2016) Development of a quantitative analysis system for greener and economically sustainable wind farms. *J Clean Prod* 133:886–898. doi:10.1016/j.jclepro.2016.06.030
7. Ardente F, Beccali M, Cellura M, Brano VL (2008) Energy performances and life cycle assessment of an Italian wind farm. *Renew Sust Energ Rev* 12(1):200–217. doi:10.1016/j.rser.2006.05.013
8. Rodríguez-Picón LA (2016) An uncertainty approach for optimization of production parameters—a case study in an extrusion molding process. *The Int J Adv Manuf Technol*:1–10. doi:10.1007/s00170-016-9358-x
9. Liu C, Li Y, Shen W (2014) Integrated manufacturing process planning and control based on intelligent agents and multi-dimension features. *The Int J Adv Manuf Technol* 75(9–12):1457–1471. doi:10.1007/s00170-014-6246-0

10. Chu W, Li Y, Liu C, Mou W, Tang L (2014) A manufacturing resource allocation method with knowledge-based fuzzy comprehensive evaluation for aircraft structural parts. *Int J Prod Res* 52(11):3239–3258. doi:[10.1080/00207543.2013.869369](https://doi.org/10.1080/00207543.2013.869369)
11. Li Y, Liu X, Gao JX, Maropoulos PG (2012) A dynamic feature information model for integrated manufacturing planning and optimization. *CIRP Ann Manuf Technol* 61(1):167–170. doi:[10.1016/j.cirp.2012.03.085](https://doi.org/10.1016/j.cirp.2012.03.085)
12. Maropoulos PG, Bramall DG, Chapman P, Cheung WM, McKay KR, Rogers BC (2006) Digital enterprise technology in production networks. *The Int J Adv Manuf Technol* 30(9–10):911–916. doi:[10.1007/s00170-005-0063-4](https://doi.org/10.1007/s00170-005-0063-4)
13. Martínez E, Sanz F, Pellegrini S, Jiménez E, Blanco J (2009) Life-cycle assessment of a 2-MW rated power wind turbine: CML method. *The Int J Life Cycle Assess* 14(1):52–63. doi:[10.1007/s11367-008-0033-9](https://doi.org/10.1007/s11367-008-0033-9)
14. Oebels KB, Pacca S (2013) Life cycle assessment of an onshore wind farm located at the northeastern coast of Brazil. *Renew Energy* 53:60–70. doi:[10.1016/j.renene.2012.10.026](https://doi.org/10.1016/j.renene.2012.10.026)
15. Hammond G, Jones C (2011) Inventory of carbon & energy version 2.0 (ICE V2. 0). Department of Mechanical Engineering, University of Bath, Bath, UK
16. Lloyd SM, Ries R (2007) Characterizing, propagating, and analyzing uncertainty in life cycle assessment: a survey of quantitative approaches. *J Ind Ecology* 11(1):161–179. doi:[10.1162/jiec.2007.1136](https://doi.org/10.1162/jiec.2007.1136)
17. Sugiyama H, Fukushima Y, Hirao M, Hellweg S, Hungerbühler K (2005) Using standard statistics to consider uncertainty in industry-based life cycle inventory databases. *The Int J Life Cycle Assess* 10(6):399–405. doi:[10.1065/lca2005.05.211](https://doi.org/10.1065/lca2005.05.211)
18. Wang E, Shen Z (2003) A hybrid data quality indicator and statistical method for improving uncertainty analysis in LCA of complex system: application to the whole-building embodied energy analysis. *J Clean Prod* 43:166–173. doi:[10.1016/j.jclepro.2012.12.010](https://doi.org/10.1016/j.jclepro.2012.12.010)
19. Huijbregts MA (1998) Application of uncertainty and variability in LCA. *The Int J Life Cycle Assess* 3(5):273–280. doi:[10.1007/BF02979835](https://doi.org/10.1007/BF02979835)
20. Kabir MR, Rooke B, Dassanayake GM, Fleck BA (2012) Comparative life cycle energy, emission, and economic analysis of 100 kW nameplate wind power generation. *Renew Energy* 37(1):133–141. doi:[10.1016/j.renene.2011.06.003](https://doi.org/10.1016/j.renene.2011.06.003)
21. Tan RR, Culaba AB, Purvis MR (2002) Application of possibility theory in the lifecycle inventory assessment of biofuels. *Int J Energy Res* 26(8):737–745. doi:[10.1002/er.812](https://doi.org/10.1002/er.812)
22. Fleck B, Huot M (2009) Comparative life-cycle assessment of a small wind turbine for residential off-grid use. *Renew Energy* 34(12):2688–2696. doi:[10.1016/j.renene.2009.06.016](https://doi.org/10.1016/j.renene.2009.06.016)
23. Khan FI, Hawboldt K, Iqbal MT (2005) Life cycle analysis of wind-fuel cell integrated system. *Renew Energy* 30(2):157–177. doi:[10.1016/j.renene.2004.05.009](https://doi.org/10.1016/j.renene.2004.05.009)
24. Ortiz O, Castells F, Sonnemann G (2009) Sustainability in the construction industry: a review of recent developments based on LCA. *Constr Build Mater* 23(1):28–39. doi:[10.1016/j.conbuildmat.2007.11.012](https://doi.org/10.1016/j.conbuildmat.2007.11.012)
25. Wang Y, Sun T (2012) Life cycle assessment of CO2 emissions from wind power plants: methodology and case studies. *Renew Energy* 43:30–36. doi:[10.1016/j.renene.2011.12.017](https://doi.org/10.1016/j.renene.2011.12.017)
26. Weidema BP, Wesnaes MS (1996) Data quality management for life cycle inventories—an example of using data quality indicators. *J Clean Prod* 4(3):167–174. doi:[10.1016/S0959-6526\(96\)00043-1](https://doi.org/10.1016/S0959-6526(96)00043-1)
27. NETL (2010) Life cycle inventory data—unit process: horizontal turbine main frame, 1.5–6 MW capacity, manufacturing. U.S. Department of Energy, National Energy Technology Laboratory, 2010. Last Updated: November 2010 (version 01). [www.netl.doe.gov/energy-analyses](http://www.netl.doe.gov/energy-analyses), <http://www.netl.doe.gov/energy-analyses>. (Accessed on 26-07-2016)
28. Canter KG, Kennedy DJ, Montgomery DC, Keats JB, Carlyle WM (2002) Screening stochastic life cycle assessment inventory models. *The Int J Life Cycle Assess* 7(1):18–26. doi:[10.1007/BF02978906](https://doi.org/10.1007/BF02978906)
29. NETL (2010) Life cycle inventory data—unit process: horizontal turbine main frame, 1.5–6 MW capacity, manufacturing. U.S. Department of Energy, National Energy Technology Laboratory. Last Updated: November 2010 (version 01). [www.netl.doe.gov/energy-analyses](http://www.netl.doe.gov/energy-analyses). (accessed on 26-07-2016)
30. Cohen J, Schweizer T, Laxson A, Butterfield S, Schreck S, Fingersh L, Veers P, Ashwill T (2008) Technology improvement opportunities for low wind speed turbines and implications for cost of energy reduction. National Renewable Energy Laboratory, Golden, Colorado (US), Technical Report NREL/TP-500-41036
31. Lantz E, Wiser R, Hand M (2012) IEA Wind Task 26: the past and future cost of wind energy, work package 2. National Renewable Energy Laboratory (NREL), Golden, CO
32. Papadopoulos I (2010) Comparative analysis of electricity generating technologies with regards to environmental burdens. PhD Dissertation, University of Bath, UK
33. Fingersh LJ, Hand MM, Laxson AS (2006) Wind turbine design cost and scaling model. National Renewable Energy Laboratory Golden, CO.
34. Venkatesh A, Jaramillo P, Griffin WM, Matthews HS (2010) Uncertainty analysis of life cycle greenhouse gas emissions from petroleum-based fuels and impacts on low carbon fuel policies. *Environ Sci Technol* 45(1):125–131. doi:[10.1021/es102498a](https://doi.org/10.1021/es102498a)